Available online at www.sciencedirect.com
SCIENCE DIRECT®
International Journal of Heat and Mass Transfer 47 (2004) 5407–5416
International Journal of HEAT and MASS TRANSFER
www.elsevier.com/locate/ijhmt

Convection in laminar three-dimensional separated flow

J.H. Nie, B.F. Armaly *

Department of Mechanical and Aerospace Engineering and Engineering Mechanics, University of Missouri—Rolla, Rolla, MO 65401, USA

Received 12 March 2004; received in revised form 14 July 2004
Available online 16 September 2004

Abstract

Distributions of the wall temperature, the Nusselt number, and the friction coefficient on all of the bounding walls of laminar three-dimensional forced convection flow adjacent to backward-facing step in a rectangular duct are reported. A uniform heat flux is imposed on the bounding walls (stepped wall, sidewalls, and flat wall) downstream from the step, while the walls of the duct upstream from the step and the step are treated as adiabatic surfaces. The flow upstream of the step is treated as hydrodynamically fully developed and isothermal, and the outlet flow downstream from the step is treated as being hydrodynamically and thermally fully developed. Local and average results are presented for a Reynolds numbers range of 150–450, and some results are compared with their equivalent from the two-dimensional case.

1. Introduction

Flow separation followed by reattachment due to sudden expansion in geometry, such as in a backward-facing step flow, occurs in numerous heat exchanging devices. Some two-dimensional (2-D) [1–5], and three-dimensional (3-D) [6–11] studies have been published on convective heat transfer in separated-reattached flow using the backward-facing step geometry in a rectangular duct. In most of these studies, the bottom stepped wall is heated while the other walls are treated as adiabatic surfaces, and wall temperature or heat transfer results are presented only for the stepped wall. For the case where the geometry is two-dimensional (a duct with large aspect ratio), there is little interest in what is the heat transfer distribution on the other walls because the flow separation, recirculation, and reattachment occurs only adjacent to the stepped wall. For the 3-D separated-reattached convection flow (a duct with small aspect ratio), however, reverse flow regions develop adjacent to all of the bounding walls (the sidewalls, the stepped wall, and the flat wall) downstream from the step [6,7], and that influences significantly the distributions of the temperature and the heat transfer from these walls. Since three-dimensional flow develops in most of the heat exchanging devices, and since all of the bounding walls are normally heated in these devices, knowledge of the temperature, Nusselt number, and friction coefficient distributions on all of the bounding walls is useful for design optimization. To the authors' knowledge, such results have not been published in the literature, and that motivated the present study.

2. Problem statement and simulation procedures

Three-dimensional laminar forced convection flow adjacent to backward-facing step in a rectangular duct

* Corresponding author. Tel.: +1 573 341 4601; fax: +1 573 341 4607.
E-mail address: armaly@umr.edu (B.F. Armaly).

0017-9310/$ - see front matter © 2004 Elsevier Ltd. All rights reserved.
doi:10.1016/j.ijheatmasstransfer.2004.07.030

Nomenclature

AR	aspect ratio, W/h
b	height or width of one bounding wall
C_f	skin friction coefficient, $2\tau_w/\rho u_0^2$
C_p	specific heat
ER	expansion ratio, H/h
H	duct's height downstream of the step
h	duct's height upstream of the step
k	thermal conductivity
L	half width of the duct, $W/2$
n	normal direction to the wall
$\overline{Nu}$	streamwise average Nusselt number, $q_w S/(\overline{T}_w - \overline{T}_b)$
Nu_a	spanwise average Nusselt number on one bounding wall, $q_w S/k(T_{wa} - T_b)$
Nu_b	bulk Nusselt number, $q_w S/k(T_{w,avg} - T_b)$
q_w	local wall heat flux, $-k\frac{\partial T}{\partial n}\|_{\text{at the wall}}$
Re	Reynolds number, $2\rho u_0 h/\mu$
S	step height
T	temperature
T_0	inlet temperature
T_b	local bulk temperate, $\frac{\int_0^W\int_0^H \rho C_p u(x,y,z)T(x,y,z)\,dy\,dz}{\int_0^W\int_0^H \rho C_p u(x,y,z)\,dy\,dz}$
T_w	local wall temperature
$T_{w,avg}$	average walls temperature, $\frac{1}{(2L+H)}(\int_0^L T_{w,step}\,dz + \int_0^H T_{w,side}\,dy + \int_0^L T_{w,flat}\,dz)$
T_{wa}	average temperature for one bounding wall, $\frac{1}{b}\int_0^b T_w\,ds$
$\overline{T}_b$	streamwise average bulk temperature $= \frac{\int_0^x\int_0^H\int_0^L \rho C_p u(x,y,z)\cdot T(x,y,z)\,dz\,dy\,dx}{\int_0^x\int_0^H\int_0^L \rho C_p u(x,y,z)\,dz\,dy\,dx}$
$\overline{T}_w$	streamwise average walls temperature, $\frac{1}{x(2L+H)}\{\int_0^x[\int_0^L T_{w,stepwall}(x,z)\,dz + \int_0^H T_{w,sidewall}(x,y)\,dy + \int_0^L T_{w,flatwall}(x,z)\,dz]\,dx\}$
u	streamwise velocity component
u_0	average inlet velocity
v	transverse velocity component
W	width of the duct
w	spanwise velocity component
x	streamwise coordinate axis
$x_{T_{w,min}}$	locations where the wall temperature is a minimum
x_u	locations where the streamwise velocity component is equal to zero
y	transverse coordinate axis
z	spanwise coordinate axis

Greek symbols

μ	dynamic viscosity
ρ	density
τ_w	wall shear stress, $\mu\sqrt{(\partial u/\partial y)^2 + (\partial w/\partial y)^2}$ at the flat wall and at the stepped wall; and $\mu\sqrt{(\partial u/\partial z)^2 + (\partial v/\partial z)^2}$ at the sidewall

is numerically simulated, and a schematic of the computational domain is presented in Fig. 1. The backward-facing step geometry has a step height (S) of 0.01 m and a width (W) of 0.08 m. The duct's heights upstream (h) and downstream (H) of the step are kept at 0.01 m and 0.02 m, respectively. This provides a geometry with an aspect ratio (AR = W/h) of eight and an expansion ratio (ER = H/h) of two. By exploiting the symmetry of the flow and temperature fields in the spanwise direction, the width of the computation domain was reduced to half of the actual width of the duct (L = 0.04 m). The length of the computational domain is either 0.5 m or 4.00 m downstream and 0.02 m upstream of the step respectively, i.e. $-2 \leqslant x/S \leqslant 50$ or 400. The longer calculation domain ($-2 \leqslant x/S \leqslant 400$) was used in order to obtain the asymptotic behavior for the fully developed regime downstream from the step and the shorter calculation domain ($-2 \leqslant x/S \leqslant 50$) was used for all of the results that are presented within that region. A grid of $200(x) \times 36(y) \times 36(z)$ is used for the shorter computation domain and a grid of $500(x) \times 36(y) \times 36(z)$ is used for the longer computation domain. The results from the longer calculation domain compared very well with the results from the shorter calculation domain, but required considerably larger number of grid points, more interations and more computational time. No reverse flow is observed after $x/S > 50$, and using a longer domain does not influence the results adjacent to the step for $x/S < 20$. The origin of the coordinates system is located at the bottom corner of the step where the

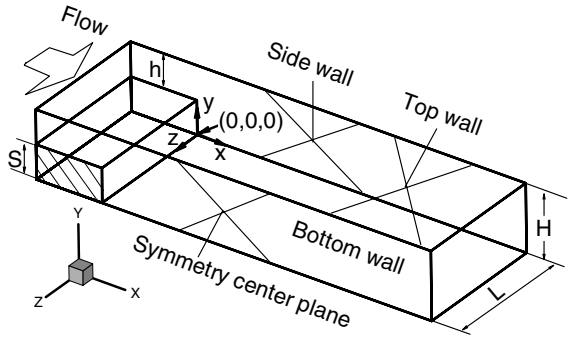

Fig. 1. Schematic of the backward-facing step geometry.

sidewall, the backward-facing step, and the stepped wall, intersect as shown in Fig. 1. The coordinate directions are also included in the figure. The steady laminar three-dimensional Navier–Stokes and energy equations are solved numerically together with the continuity equation using the finite volume method to simulate the thermal and the flow fields.

Continuity equation:

$$\frac{\partial}{\partial x}(\rho u)+\frac{\partial}{\partial y}(\rho v)+\frac{\partial}{\partial z}(\rho w)=0 \tag{1}$$

Momentum equations:

$$\frac{\partial}{\partial x}(\rho u^2)+\frac{\partial}{\partial y}(\rho uv)+\frac{\partial}{\partial z}(\rho uw) = -\frac{\partial p}{\partial x}+\mu\left(\frac{\partial^2 u}{\partial x^2}+\frac{\partial^2 u}{\partial y^2}+\frac{\partial^2 u}{\partial z^2}\right) \tag{2}$$

$$\frac{\partial}{\partial x}(\rho uv)+\frac{\partial}{\partial y}(\rho v^2)+\frac{\partial}{\partial z}(\rho vw) = -\frac{\partial p}{\partial y}+\mu\left(\frac{\partial^2 v}{\partial x^2}+\frac{\partial^2 v}{\partial y^2}+\frac{\partial^2 v}{\partial z^2}\right) \tag{3}$$

$$\frac{\partial}{\partial x}(\rho uw)+\frac{\partial}{\partial y}(\rho vw)+\frac{\partial}{\partial z}(\rho w^2) = -\frac{\partial p}{\partial z}+\mu\left(\frac{\partial^2 w}{\partial x^2}+\frac{\partial^2 w}{\partial y^2}+\frac{\partial^2 w}{\partial z^2}\right) \tag{4}$$

Energy equation:

$$\frac{\partial}{\partial x}(\rho C_p uT)+\frac{\partial}{\partial y}(\rho C_p vT)+\frac{\partial}{\partial z}(\rho C_p wT) = k\left(\frac{\partial^2 T}{\partial x^2}+\frac{\partial^2 T}{\partial y^2}+\frac{\partial^2 T}{\partial z^2}\right) \tag{5}$$

The physical properties are treated as constants and evaluated for air at the inlet temperature (T_0) of 20 °C, that is, density (ρ) is 1.205 kg/m^3, specific heat (C_p) is 1005 J/(kg °C), dynamic viscosity (μ) is 1.81×10^{-5} kg/(m s), and thermal conductivity (k) is 0.0259 W/(m °C). Flow at the inlet section upstream of the step ($x/S=-2$) is considered to be isothermal ($T_0=20$ °C), hydrodynamically steady and fully developed with a distribution for the streamwise velocity component (u) equal to the one described by Shah and London [12] for fully developed flow in a rectangular duct. The other two velocity components, v and w, are set to be equal to zero at that inlet section. No slip boundary condition (zero velocities) is applied to all of the wall surfaces. Uniform and constant heat flux of $q_w=20$ W/m^2 is specified at all the bounding walls downstream from the step, i.e. the stepped wall ($0<x/S\leqslant 50$ or 400, $y/S=0$ and $0\leqslant z/L\leqslant 1$); the flat wall ($0<x/S\leqslant 50$ or 400, $y/S=2$ and $0\leqslant z/L\leqslant 1$); and the sidewalls ($0<x/S\leqslant 50$ or 400, $0\leqslant y/S\leqslant 2$ and $z/L=0$ and 2), while the other walls upstream from the step and the backward-facing step are treated as adiabatic surfaces. Fully developed flow and thermal boundary conditions are imposed at the exit section of the calculation domain ($x/S=50$ or 400).

The governing equations are discretized using the finite volume method, and the control volumes are located utilizing the staggered grid arrangement. The resulting finite difference equations are solved numerically by making use of a line-by-line method combined with alternating direction iteration (ADI) scheme. SIMPLE algorithm is utilized for the computation of pressure correction in the iteration procedure, and hexahedron volume elements with non-uniform grid system are employed in the simulations. The grid is highly concentrated close to the step and near the step corners, in order to insure the accuracy of the numerical simulations. This flow simulation code was used in previous studies [7,9], and its description and validation can be found in these references. The convergence criterion required that the maximum relative mass residual based on the inlet mass be smaller than 10^{-6}. It usually takes about 4000 interations to meet this requirement for the shorter domain computation, while it takes about 25,000 interations for the longer domain calculation.

3. Results and discussion

Distributions of the temperature, the average and the bulk Nusselt numbers, and the friction coefficient, on all of the bounding walls downstream from the step are presented for different Reynolds numbers ($Re=150$, 250, 343 and 450) where the flow has been verified experimentally to be laminar in this geometry. Reverse flow regions adjacent to the stepped wall, sidewalls, and flat wall develop in this geometry and the limiting streamlines on the bounding walls are presented in Fig. 2 for the Reynolds number of 150 in order to capture some of the flow features that develop adjacent to these walls. Different colors in this figure represent the magnitude of the normal velocity away from and toward each of the walls, with the red being the highest away from the wall and blue being the highest toward the wall. Similar results are available for other Reynolds numbers and exhibit similar features, but are not presented here due to space limitations. The boundary lines for the reverse flow regions that develop adjacent to these walls (the x_b-line) are identified by interpolations between two neighboring limiting streamlines that are separating two flow regions: in one region the flow is moving toward the upstream direction (i.e. the negative x-direction) and in the other region the flow is moving toward the downstream direction (i.e. the positive x-direction). The dashed black lines on this figure identify the boundaries of the reverse flow regions. This figure illustrates that a ''jet-like'' flow impinges on the stepped

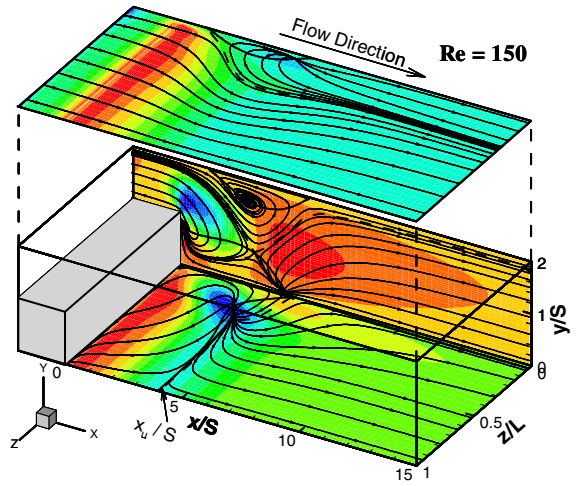

Fig. 2. Limiting streamlines adjacent to the bounding walls.

wall and a primary recirculation flow region develops adjacent to that wall; a downwash and a reverse flow region develop near the step and adjacent to the sidewall; a reverse flow region develops adjacent to the sidewall and near the flat wall; and a reverse flow region develops adjacent to the flat wall near the sidewall. The solid black lines that are included in this figure represent the locations where the streamwise component of wall shear stress is zero (the x_u-line), and it also represents the boundary where the streamwise velocity component (u) changes direction, i.e. identifying the points where the reverse flow occurs in the streamwise direction. Discussion of the flow behavior in this geometry has been presented by Armaly et al. [6] and Nie and Armaly [7], and will not be repeated here.

Distributions of the local wall temperature (T_w) on the stepped wall ($y/S = 0$), the sidewall ($z/L = 0$) and the flat wall ($y/S = 2$) downstream of the step ($x/S > 0$) are presented in Fig. 3 for Reynolds number equal to 343. Results for other Reynolds numbers are available but are not presented here due to space limitations, and they exhibit similar behavior as the one presented in Fig. 3. The temperature distribution on the stepped wall exhibits a maximum at the bottom corner of the step near the sidewall, and a minimum at $x/S \approx 8.5$ and $z/L \approx 0.3$ (the general region that is impacted by the reattaching "jet-like" flow [6,7]). Temperatures on that wall increase gradually as the distance from the step continues to increase beyond $x/S = 10$. The sidewall temperature distribution has a peak at the bottom corner near the step, thus matching the general location where the temperature peak occurs on the stepped wall, decreases slightly in the streamwise direction and then starts to increase gradually as the distance from the step continues to increase. The temperature of the flat wall increases in the streamwise direction, and its spanwise

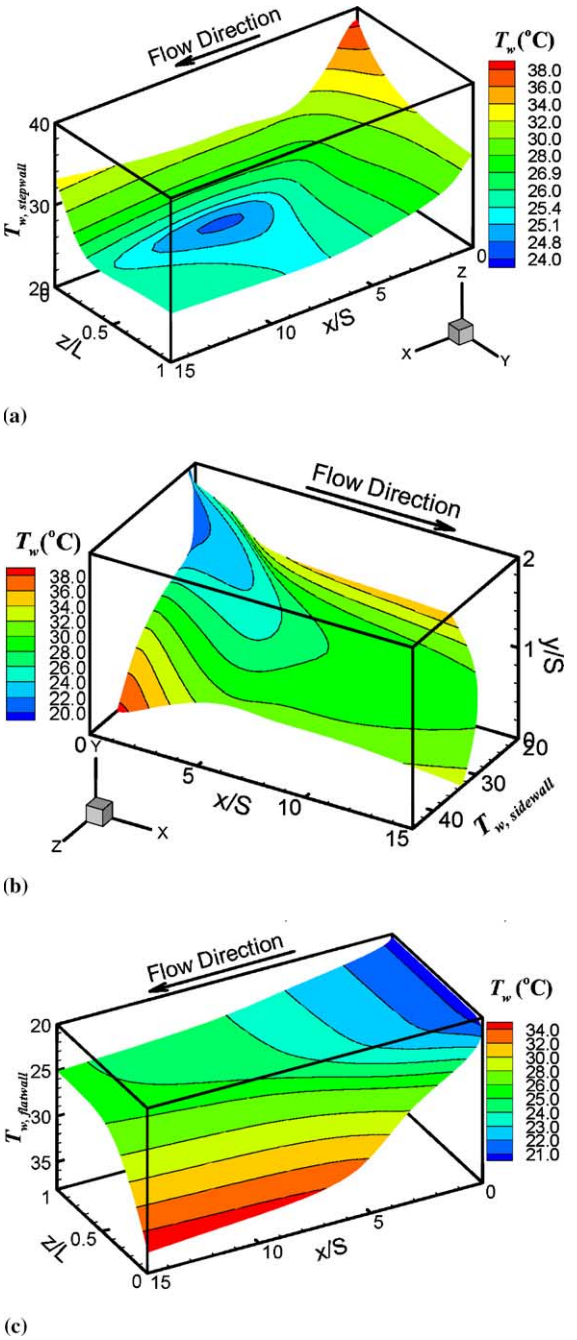

Fig. 3. Temperature distribution on the bounding walls for $Re = 343$. (a) On the stepped wall ($y/S = 0$ and $x/S > 0$). (b) On the sidewall ($z/L = 0$ and $x/S > 0$). (c) On the flat wall ($y/S = 2$ and $x/S > 0$).

behavior exhibits a minimum at the center of the duct ($z/L = 1$) and a maximum at the sidewall. The locations where the temperature is a minimum on the bounding walls are presented by the dashed lines in Fig. 4 for

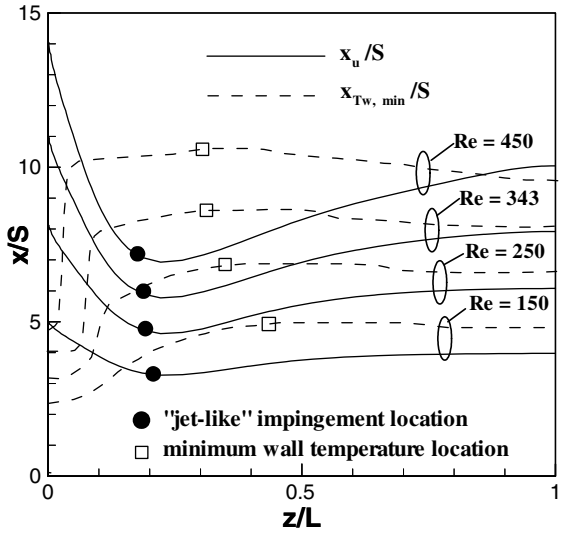

Fig. 4. Locations where the wall temperature is a minimum ($x_{T_{w,min}}$) and where the streamwise component of the wall shear stress is zero (x_u).

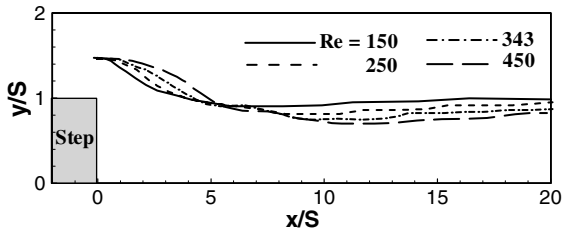

Fig. 5. Locations where the temperature on the sidewall is a minimum ($x_{T_{w,min}}$).

the stepped wall, and in Fig. 5 for the sidewall for different Reynolds numbers. Such a line is not presented for the flat wall because it is located at the symmetry centerline of the duct ($z/L = 1$ and $y/S = 2$). The solid lines in Fig. 4 represent the locations where the streamwise component of wall shear stress is zero (the x_u-line). It is interesting to note that the location where the "jet-like" flow impinges on the stepped wall (denoted by the sold circle symbol) does not coincide with the location where the wall temperature is a minimum (denoted by the square symbol). The minimum wall temperatures are located downstream from the locations where the "jet-like" flow impinges on the stepped wall (due to the relatively high spanwise flow in that region), and the distance between these two locations increases and moves further away from the step as the Reynolds number increases. The rapid drop in the stepped wall temperature near the sidewall is caused by the downwash (incoming fluid with relatively low temperature) that develops in that region.

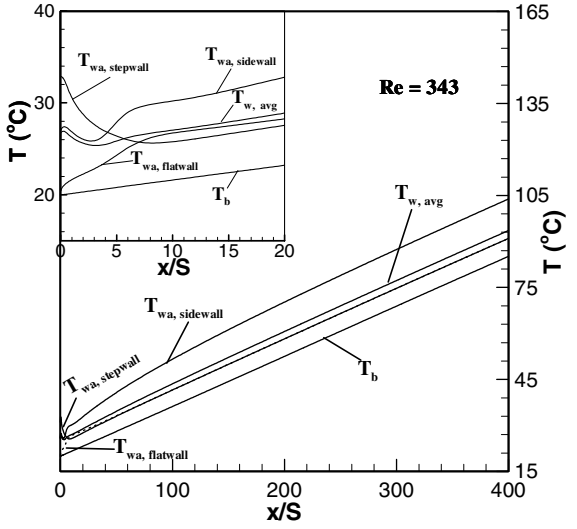

Fig. 6. Streamwise distributions of the bulk temperature and the average walls temperatures.

The location where the sidewall temperature is a minimum is approximately at the center of that wall as shown in Fig. 5 for different Reynolds numbers.

The streamwise distributions of the local bulk temperature (T_b), the average wall temperature for the bounding walls (T_{wa}), and the average wall temperature for each of the bounding walls are presented in Fig. 6. The results show that the average temperatures of the stepped wall ($T_{wa,stepwall}$) and the flat wall ($T_{wa,flatwall}$) become equal to each other at approximately $x/S = 35$ and their slopes along with the slope of the average walls temperature ($T_{w,avg}$) become equal to the bulk temperature at $x/S = 100$. The dashed line on the figure is used to represent the average temperature of the flat wall ($T_{wa,flatwall}$) in order to differentiate it from the average temperature of the stepped wall ($T_{wa,stepwall}$). The average sidewall temperature, however, does not exhibit this behavior until $x/S = 200$. The calculation domain was extended to the range of $-2 \leqslant x/S \leqslant 400$, in order to illustrate the asymptotic approach to the fully developed value. Most of the results, however, are presented only in the range of $0 \leqslant x/S \leqslant 50$ (or 20 for some results) to illustrate more clearly the behavior near the step. Distributions of the temperatures near the reattachment region can be seen more clearly from the embedded figure in Fig. 6. The average temperature of the sidewall ($T_{wa,sidewall}$) is greater than those of the stepped wall ($T_{wa,stepwall}$) and of the flat wall ($T_{wa,flatwall}$) for $x/S > 4$ for the Reynolds number of 343. A local peak develops in its distribution at $x/S \approx 8$ at this Reynolds number. This is due to the rebounding of the "jet-like" flow that impinges on the heated bottom stepped wall, and then flows adjacent to the sidewall causing its temperature

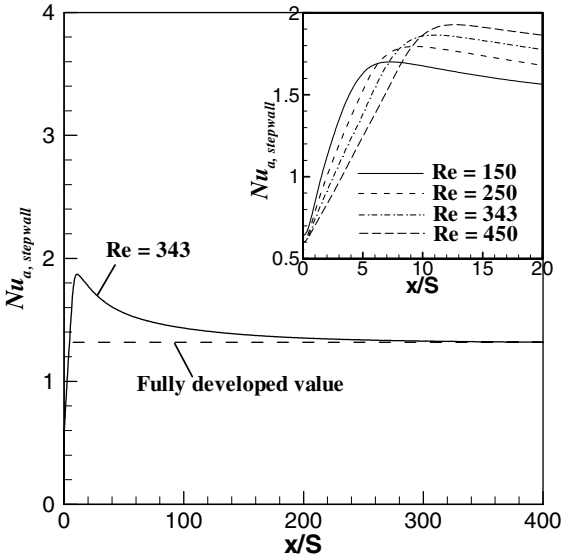

Fig. 7. Streamwise distribution of the average Nusselt number on the stepped wall.

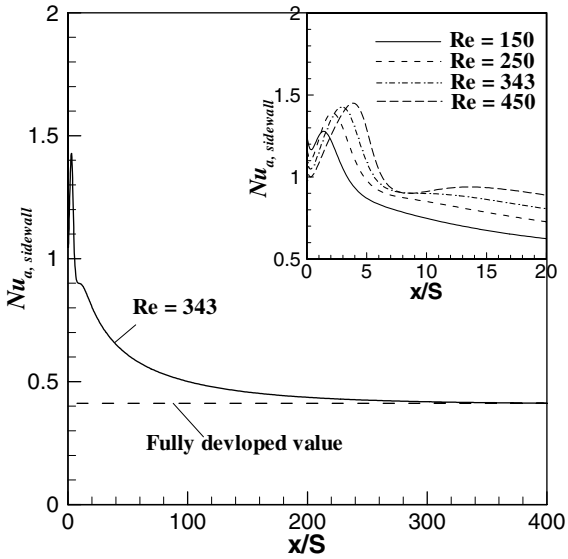

Fig. 8. Streamwise distribution of the average Nusselt number on the sidewall.

to increase. The relatively high average sidewall temperature ($T_{wa,sidewall}$) causes the overall average walls temperature ($T_{w,avg}$) to be higher than either the average temperature of the stepped wall or the flat wall for $x/S > 5.5$ at this Reynolds number.

Streamwise distributions of the average Nusselt number (Nu_a) are presented for the stepped wall in Fig. 7, for the sidewall in Fig. 8, and for the flat wall in Fig. 9 for different Reynolds numbers. A peak in the average Nusselt number distribution on the stepped wall develops (Fig. 7), and the streamwise locations where this peak occurs on the stepped wall move further downstream with the increase of Reynolds number. This Nusselt number increases with increasing Reynolds number for streamwise locations downstream from the location where the maximum occurs (downstream from the reattachment), but decreases for streamwise locations smaller than the location where the maximum occurs (upstream of the reattachment and inside the recirculation region). The fully developed values for the average Nusselt number on this wall are also shown in this figure, which is 1.316. Similar behavior is seen in the streamwise distribution of the average Nusselt number on the sidewall, which increases outside the downwash region (that develops adjacent to the sidewall near the step) and decreases inside that downwash region as the Reynolds number increases. A decrease appears to develop in the magnitude of the Nusselt number at the sidewall at $x/S \approx 8$ for Reynolds number of 450. This is due to the rebounding "jet-like" flow that causes the average sidewall temperature to increase and the average Nusselt number to decrease in that region. The location

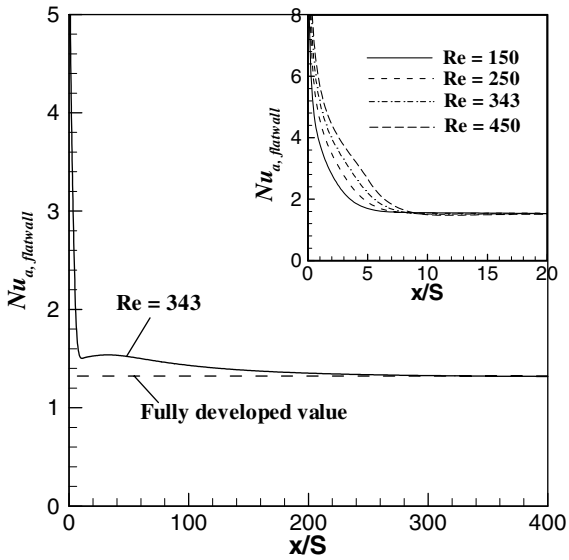

Fig. 9. Streamwise distribution of the average Nusselt number on the flat wall.

where the maximum average Nusselt number develops on the sidewall is closer to the step (approximately half of the distance) than the location where the maximum average Nusselt number develops on the stepped wall for the same Reynolds number. The former is caused by the downwash flow near the sidewall while the latter is caused by the reattaching flow on the stepped wall. The fully developed values for the average Nusselt

number on that wall are also presented in this figure, which is 0.411. The streamwise distribution of the average Nusselt number on the flat wall as shown in Fig. 9, does not exhibit any maximum and it decreases gradually as the distance from the step increases reaching asymptotically the fully developed value at relatively short distance from the step. A slightly minimum value in its distribution is observed at $x/S \approx 10$, because of the decrease of steamwise velocity component due to sudden expansion in geometry. The fully developed values for the average Nusselt number on that wall are also presented in this figure, which is 1.316. The bulk Nusselt number (Nu_b) that represents the average for all the bounding walls exhibits a behavior that is similar to the one described for the average Nusselt number on the sidewall as shown in Fig. 8, and that is due to the strong influence of the average sidewall temperature on the bulk temperature and on the average walls temperature. The asymptotic approach to the fully developed value is seen to occur at $x/S \approx 320$. The effect of the Reynolds number on the bulk Nusselt number is presented in Fig. 10, and the fully developed values are also presented in this figure.

Results from two-dimensional (2-D) simulations of backward-facing step forced convection flow for the same conditions as those performed in this paper for the 3-D case are presented in Figs. 11 and 12 for a Reynolds number of 343. The streamwise distributions of the average temperature on the stepped wall ($T_{w,stepwall}$) and on the flatwall ($T_{w,flatwall}$) for the 2-D case (in Fig. 11) have similar trend but are lower in magnitude than the results of 3-D case that are presented in Fig. 6. For the 2-D case, the notation $T_{w,stepwall}$ is equivalent to

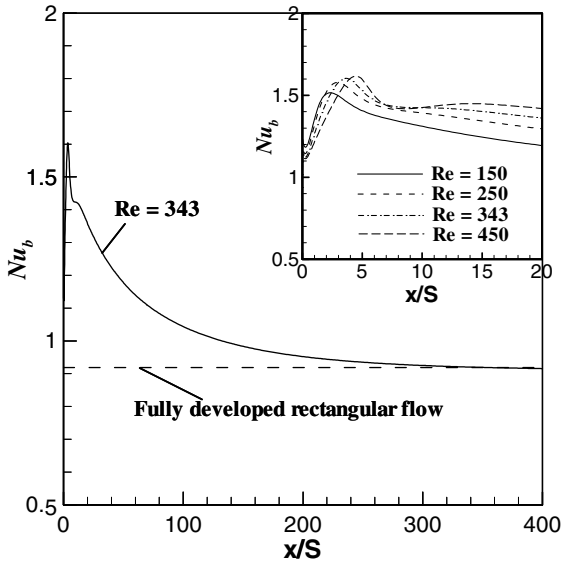

Fig. 10. Streamwise distribution of the bulk Nusselt number.

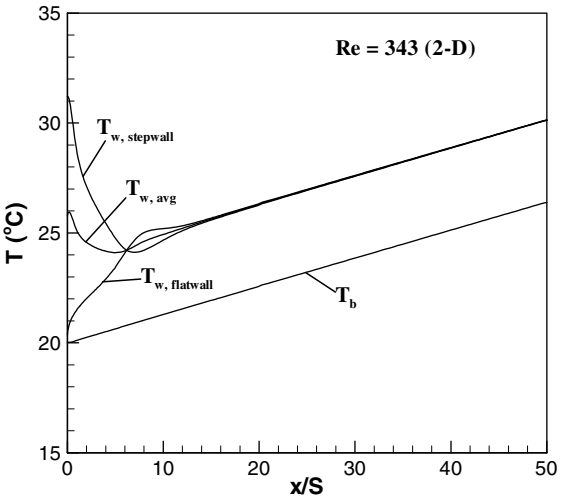

Fig. 11. Streamwise distributions of the bulk temperature and the average walls temperatures (2-D).

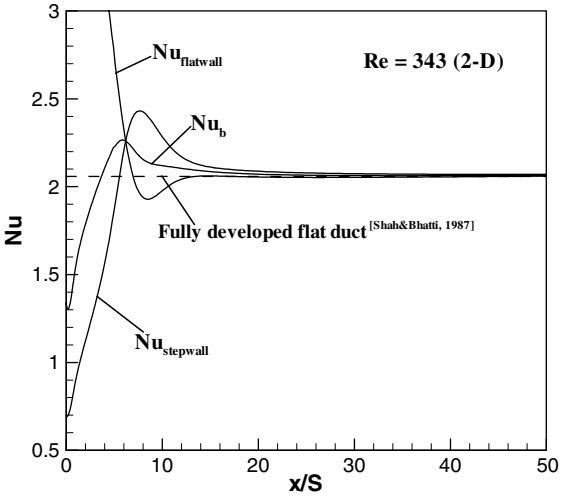

Fig. 12. Streamwise distribution of the bulk Nusselt number (2-D).

$T_{wa,stepwall}$, and $T_{w,flatwall}$ is equivalent to $T_{wa,flatwall}$ of the 3-D case. It should be noted that for the 2-D case the average walls temperature ($T_{w,avg}$) is calculated as $T_{w,avg} = (T_{w,stepwall} + T_{w,flatwall})/2$. As a result, the average walls temperature ($T_{w,avg}$) for the 2-D case is between the temperatures of the stepped wall and the flat wall. On the other hand the average walls temperature for the 3-D case (in Fig. 6) is greater than either the average stepped wall ($T_{wa,stepwall}$) or the average flat wall ($T_{wa,flatwall}$) temperatures. This is due to the supplied heat flux on the sidewall and the relatively high average temperature of the sidewall ($T_{wa,sidewall}$) which influences

significantly the average walls temperature. Streamwise distributions of the Nusselt number for the 2-D case are presented in Fig. 12, where the bulk temperature is defined as

$$T_b = \frac{\int_0^H \rho C_p u(x,y) T(x,y)\,dy}{\int_0^H \rho C_p u(x,y)\,dy}$$

The dashed line in Fig. 12 represents the Nusselt number value for the fully developed duct flow, which is 2.06 as reported by Shah and Bhatti [13]. It can be seen from the figure that the Nusselt numbers, including the Nusselt number on the stepped wall and the flat wall, and the bulk Nusselt number, asymptotically approach the fully developed value at relatively short distance from the step, i.e. $x/S \approx 30$. A peak develops in the distribution of Nusselt number of the stepped wall and a minimum develops in the distribution of Nusselt number of the flat wall at $x/S \approx 8$. The peak on the stepped wall is due to the flow reattachment on that wall, and the minimum is due to the relatively low streamwise velocity component that develops in that region of the flat wall due to the sudden expansion in geometry. It should be noted that the fully developed value for the average Nusselt number for the 2-D case (2.06) is higher than the fully developed value for the 3-D case (0.92) as seen in Figs. 10 and 12. Fig. 13 illustrates that the streamwise distributions of the average bulk Nusselt number for the 2-D case are always higher than its equivalent for the 3-D case with a peak that develops at $x/S \approx 6$. The fully developed 3-D bulk Nusselt number value will not approach the fully developed 2-D value as the aspect ratio of the duct approaches infinity (AR $\rightarrow \infty$) as noted by Shah and Bhatti [13]. This is due to the fact that the sidewall heat flux that is accounted for in the 3-D case continues to strongly influence the average wall temperature and the bulk temperature even as the aspect ratio of the duct increases and approaches infinity. The fully devel-

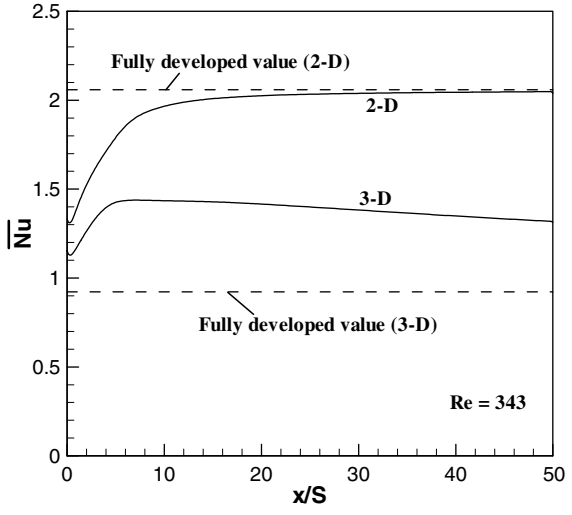

Fig. 13. Streamwise distributions of the average bulk Nusselt number.

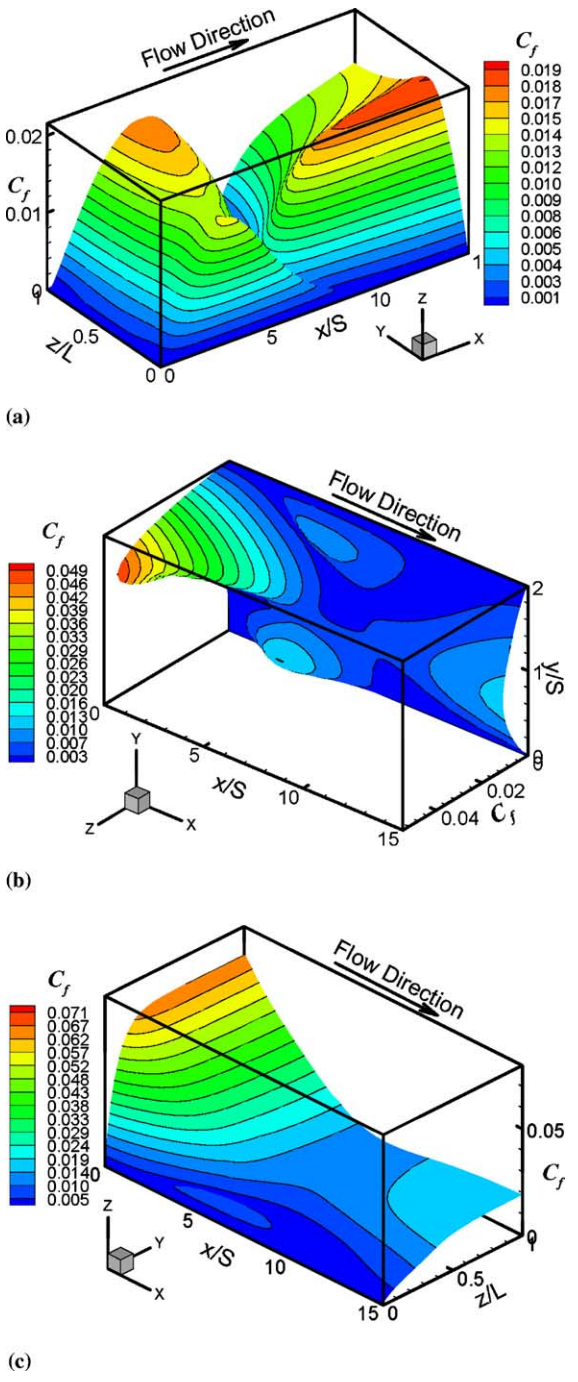

Fig. 14. Distributions of the friction coefficient for $Re = 343$. (a) On the stepped wall ($y/S = 0$ and $x/S > 0$). (b) On the sidewall ($z/L = 0$ and $x/S > 0$). (c) On the flat wall ($y/S = 2$ and $x/S > 0$).

oped values for the 2-D and the 3-D cases are also included in this figure.

Distributions of the local friction coefficient (C_f) on the bounding walls are presented in Fig. 14 for the Reynolds number of 343. The results show that the friction coefficient is relatively low along the boundaries of the reverse flow regions where the streamwise component of wall shear stress is zero. The friction coefficient inside the primary reverse flow on the stepped wall is relatively high, due to the strong vortical spanwise flow that develops adjacent to the stepped wall inside this region [6,7]. The peak that develops on that wall downstream from the primary reverse flow region is located near the sidewall and not at the center width of the duct as one would expect. Several peaks develop in the distribution of the local friction coefficient on the sidewall ($z/L = 0$). The relatively high velocity gradient near the step and the downwash that develops adjacent to the sidewall in that region are responsible for the peak that develops in that region. The other two peaks that develop on the sidewall, as seen in Fig. 14b, are associated with the reverse flow regions that develop on that wall. The distribution in the redeveloping flow region on the sidewall becomes similar to the one for a rectangular duct flow, with the peak value in the center region of the wall. The distribution on the flat wall ($y/S = 2$) develops a maximum near the step due to the relatively high velocity gradients that are caused by the sudden expansion in geometry, but that distribution becomes uniform across most of the width of the duct in that region. Near the sidewall and in the reverse flow region that develops on that flat wall, the friction coefficient is relatively low but it exhibits a relative maximum at the center of that reverse flow region. The friction coefficient on the flat wall decreases rapidly to a minimum along the streamwise direction at the center of the duct, and starts to gradually increase as the distance from the step continues to increase exhibiting the expected behavior of a flow in a duct.

4. Conclusions

Convection in three-dimensional laminar, forced, separated-reattached flow adjacent to backward-facing step in a rectangular duct, where all bounding walls are heated with constant heat flux, is examined for the purpose of determining the flow and thermal behavior that develops in this geometry with these boundary conditions. The locations where the wall temperature is a minimum and where the "jet-like" flow impinges on the stepped wall move further downstream from the step as the Reynolds number increases. The minimum wall temperature is located downstream from the location where the "jet-like" flow impinges on the stepped wall. The average bounding walls temperature ($T_{w,avg}$) downstream of the reattachment is higher than the average wall temperature of either the stepped wall or the flat wall, due to the relatively high average temperature of the sidewall. The average Nusselt numbers on the stepped wall and on the sidewall exhibit a maximum in their streamwise distributions and the location where that maximum occurs moves away from the step as the Reynolds number increases. The location where the average Nusselt number is a maximum on the sidewall is closer to the step (approximately half of the distance) than the location where the maximum is located on the stepped wall for the same Reynolds number. The average Nusselt number on the flat wall decreases gradually along the streamwise direction reaching asymptotically the fully developed value. The bulk Nusselt number exhibits a behavior that is similar to the one for the sidewall due to the strong influence of the average sidewall temperature on the bulk and on the average walls temperature. The average bulk Nusselt number for the 2-D case is higher than that for the 3-D case, and the fully developed 3-D value will not approach the 2-D fully developed value as the aspect ratio of the duct increases and approaches infinity ($AR \rightarrow \infty$). The results for the 2-D case start to approach the fully developed values at relatively short distance from the step ($x/S = 30$), but the 3-D case requires much longer distance ($x/S = 170$) to approach the fully developed results. The friction coefficient inside the primary reverse flow is relatively high, due to the strong vortical spanwise flow that develops adjacent to the stepped wall inside this region. The peak in the friction coefficient downstream of the primary reverse flow region on the stepped wall is located near the sidewall and not at the center width of the duct as one would expect. Several peaks develop in the distribution of the local friction coefficient on the sidewall: the first is due to the relatively high velocity gradient near the step; the second is due to the downwash that develops adjacent to the sidewall; and the third is due to the reverse flow regions that develop on that upper portion of that wall. The friction coefficient has a maximum near the step due to the relatively high velocity gradients that are caused by the sudden expansion in geometry, and its distribution is almost uniform across most of the width of the duct in that region.

Acknowledgment

This work was supported in part by a DOE-Basic Energy Sciences Grant No. DE-FG02-03ER46067.

References

[1] R.L. Simpson, Aspects of turbulent boundary-layer separation, Progr. Aerospace Sci. 32 (5) (1996) 457–521.

[2] J.K. Eaton, J.P. Johnson, A review of research on subsonic turbulent flow reattachment, AIAA J. 19 (9) (1981) 1093–1100.
[3] B.F. Armaly, F. Durst, J.C.F. Pereira, B. Schonung, Experimental and theoretical investigation of backward-facing step flow, J. Fluid Mech. 127 (1983) 473–496.
[4] B.F. Blackwell, D.W. Pepper (Eds.), Benchmark Problems for Heat Transfer Codes, ASME HTD, 222, New York, 1992.
[5] B.F. Blackwell, B.F. Armaly (Eds.), Computational Aspects of Heat Transfer—Benchmark Problems, ASME HTD, 258, New York, 1993.
[6] B.F. Armaly, A. Li, J.H. Nie, Three-dimensional forced convection flow adjacent to backward-facing step, AIAA J. Thermophys. Heat Transfer 16 (2) (2002) 222–227.
[7] J.H. Nie, B.F. Armaly, Reattachment of three-dimensional flow adjacent to backward-facing step, ASME J. Heat Transfer 125 (3) (2003) 422–428.
[8] H. Iwai, K. Nakabe, K. Suzuki, Flow and heat transfer characteristics of backward-facing step laminar flow in a rectangular duct, Int. J. Heat Mass Transfer 43 (3) (2000) 457–471.
[9] J.H. Nie, B.F. Armaly, Three-dimensional convective flow adjacent to backward-facing step—effects of step height, Int. J. Heat Mass Transfer 45 (12) (2002) 2431–2438.
[10] J.H. Nie, B.F. Armaly, Effects of buoyancy on three-dimensional convection flow adjacent to backward-facing step, AIAA J. Thermophys. Heat Transfer 17 (1) (2003) 122–126.
[11] D.W. Pepper, D.B. Carrington, Convective heat transfer over a 3-D backward facing step, in: Proceedings of the ICHMT International Symposium on Advances in Computational Heat Transfer, Cesme, Turkey, May 26–30, 1997, pp. 273–281.
[12] R.K. Shah, A.L. London, Laminar Forced Convection in Ducts, Academic Press, New York, 1978, pp. 196–198.
[13] R.K. Shah, M.S. Bhatti, Laminar convection heat transfer in ducts, in: S. Kakac, R.K. Shah, W. Aung (Eds.), Handbook of Single-Phase Convective Heat Transfer, John Wiley & Sons, New York, 1987, pp. 3.30–3.49.